



Fabrication and application of targeted ciprofloxacin nanocarriers for the treatment of chronic bacterial prostatitis

Sahar I. Mohammad^{a,1}, Basmah Nasser Aldosari^{b,1}, Magda M. Mehanni^c, Ahmed O. El-Gendy^d, Walaa G. Hozayen^e, Obaid Afzal^f, Randa Mohammed Zaki^{g,h,*}, Ossama M. Sayedⁱ

^a Biotechnology and Life Science Department, Faculty of Postgraduate Studies for Advanced Science, Beni-Suef University, Beni-Suef, Egypt

^b Department of Pharmaceutics, College of Pharmacy, King Saud University, P.O. Box 2457, Riyadh 11451, Saudi Arabia

^c Department of Botany and Microbiology, Faculty of Science, Minia University, Minia, Egypt

^d Microbiology and Immunology Department, Faculty of Pharmacy, Beni-Suef University, Beni-Suef, Egypt

^e Biochemistry Department, Faculty of Science, Beni-Suef University, Beni-Suef, Egypt

^f Department of Pharmaceutical Chemistry, College of Pharmacy, Prince Sattam Bin Abdulaziz University, Al Kharj 11942, Saudi Arabia

^g Department of Pharmaceutics, Faculty of Pharmacy, Prince Sattam Bin Abdulaziz University, P.O. Box 173, Al-Kharj 11942, Saudi Arabia

^h Department of Pharmaceutics and Industrial Pharmacy, College of Pharmacy, Beni-Suef University, Beni-Suef 62514, Egypt

ⁱ Department of Pharmaceutics, Faculty of Pharmacy, Sinai University-Kantara Branch, Ismailia 41612, Egypt

ARTICLE INFO

Keywords:

Chronic bacterial prostatitis
Transferosomes
Monoclonal Antibody IgG
Polyethylene glycol-6 stearate
Nanoparticles
Drug targeting

ABSTRACT

Pathogenic bacteria cause chronic bacterial prostatitis (CBP). CPB is characterized by urinary tract infection and persistence of pathogenic bacteria in prostatic secretion. Owing to poor blood supply to the prostate gland and limited drug penetration, CBP treatment is difficult. Transferosomes are ultra-deformable vesicles for nanocarrier applications, which have become an important area of nanomedicine. Such carriers are specifically targeted to the pathological area to provide maximum therapeutic efficacy. It consists of a lipid bilayer soybean lecithin phosphatidylcholine (PC), an edge activator Tween 80 with various ratios, and a chloroform/methanol core. Depending on the lipophilicity of the active substance, it can be encapsulated within the core or among the lipid bilayer. Due to their exceptional flexibility, which enables them to squeeze themselves through narrow pores that are significantly smaller than their size, they can be a solution. One formulation (Cipro5 PEG) was selected for further in vitro analysis and was composed of phosphatidylcholine (PC), Tween 80, and polyethylene glycol-6 stearate (PEG-6 stearate) in a ratio of 3:3:1 in a chloroform/methanol mixture (1:2 v/v). In vitro, the results showed that PEGylated transferosomes had faster drug release, higher permeation, and increased bioavailability. The transferosomes were quantified with a particle size of 202.59 nm, a zeta potential of -49.38 mV, and a drug entrapment efficiency of 80.05%. The aim of this study was to investigate drug targeting. Therefore, Monoclonal antibody IgG was coupled with Cipro5 PEG, which has specificity and selectivity for conjugated nanoparticles. In vivo, a total of twenty-five adult Wistar rats were obtained and randomly divided into 5 groups, each of 5 rats at random: the control group, blank group, positive control group, Cipro 5PEG group, and Cipro 5PEG coupled with IgG antibody group. The cytokines levels (IL-1 β , IL-8, and TNF- α) in the serum were detected by analysis kits. Compared with the control group, treatment with Cipro 5PEG coupled with the IgG antibody could significantly inhibit cytokines, according to histological analysis. Cipro 5PEG, coupled with the IgG antibody group, reduced prostate tissue inflammation. Hence, our results show a promising approach to delivering antibiotics for the targeted therapy of CBP.

1. Introduction

Chronic bacterial prostatitis (CBP) is the most frequent cause of

relapsing UTI in men and is distinguished by recurrent UTI and persistent pathogenic bacteria in prostatic secretions (Pfau, 1986). Several clinical signs and symptoms of chronic bacterial prostatitis, including

* Corresponding authors.

E-mail address: r.abdelrahman@psau.edu.sa (R.M. Zaki).

¹ These authors contributed equally to this work.

pelvic pain and discomfort, atypical urination, sexual dysfunction, dizziness, headaches, and depression, can have an unfavorable effect on a patient's quality of life (Santharam et al., 2019). Bacterial prostatitis is a condition in which the prostate gland becomes inflamed owing to bacterial infection. Most researchers consider *E. coli*, *Enterobacter* spp., and *Pseudomonas aeruginosa* as the main pathogenic agents for 65–80% of these illnesses (Busetto et al., 2014; Shulyak et al., 2019). Compared to controls, the expression of the inflammatory protein interleukin 1 β (1 L-1 β) is greater in patients with CBP (Guo et al., 2012). The diagnosis of bacterial prostatitis is made by physical examination, urine analysis, and sometimes prostate biopsy. Some studies have shown a connection between prostatitis and prostate cancer. The high prevalence of prostatitis could contribute to prostate carcinogenesis, which is the most common malignancy among elderly men in the United States and the second most common cause of cancer-related death in males (Gregorio et al., 2006). Inflammatory mediators can promote prostatic carcinogenesis via multiple signalling pathways. Some examples include inhibiting apoptosis, promoting cell proliferation, and inducing tumor suppressor gene loss (Jiang et al., 2013). The treatment of chronic bacterial prostatitis (CBP) is challenging because of the difficulty in penetrating the prostatitis microenvironment and in delivering drugs to the prostate gland, which has a poor blood supply, limited drug penetration, inflammatory hyperplasia, high pH, bacterial accumulation, and a defect in the blood-prostate barrier (El Meliegy and Torky, 2015; Zheng et al., 2022). The main objective of antibiotic therapy is to eliminate the uropathogenic factor that causes the infection; however, when inflammation disappears, the antibiotic concentrations that may be reached in prostatic tissue run out, which makes it more difficult to achieve this goal (Charalabopoulos et al., 2003). In contrast to the acidic pH of the prostatic fluids of healthy males, prostate secretions of patients with chronic bacterial prostatitis had an alkaline pH. Quinolones such as ciprofloxacin are zwitterions that can be concentrated in both alkaline and acidic prostatic fluids (Dalhoff and Weidner, 1988; Naber et al., 1989), have a broad antibacterial spectrum, and exhibit strong activity, particularly against Enterobacteriaceae (Naber, 1989). The therapeutic efficiency of drugs should be increased while minimizing unfavorable side effects (toxic effects) through targeted delivery of drugs to the site of action. In several instances, a drug is quickly metabolized or eliminated, or has little opportunity to reach the area where it is supposed to work. In other cases, the drug freely circulates throughout the body; however, in addition to acting on the intended target site, it also has undesired side effects on tissues that are not the intended target site. When targeted, a drug is permanently attached to a pharmacologically inactive and biodegradable carrier molecule.

Nanomedicines have been established in recent years because of their many advantages such as less frequent dosing, fewer side effects, better targeting, and enhanced pharmacological qualities (Zhang and Zhang, 2020). In 1992, Cevc et al. developed a new type of drug delivery vesicle called a "transferosome," which is composed of phospholipid and a single-chain surfactant. The edge activator EA, a single-chain surfactant that weakens the phospholipid bilayer, makes the vesicle ultra-deformable and has the ability to self-optimize and self-regulate, giving this vesicle its greatest strength (Vikas et al., 2011; Walve et al., 2011). Therefore, because transferosomes are elastic in nature, they can deform and squeeze themselves into fully assembled vesicles through tiny pores that are much smaller than the vesicle size without undergoing any visible damage (Sachan et al., 2013; Sivannarayana et al., 2012). It can pass through pores smaller than its own size. Despite passing through the narrower pores, the transferosomes were able to preserve their diameters against fragmentation due to EA, which facilitated the solubilization of hydrophobic drugs and increased the entrapment efficiency of the drug (Lei et al., 2013; Pandey et al., 2014). Transferosomes have shown good colloidal stability for up to three months at both 40 °C and 25 °C (Hadidi et al., 2018). Using "stealthy" molecules is a suitable method for extending the in vivo circulation lifespan of drug carriers. A stealthy modified carrier can avoid being

recognized by the mononuclear phagocyte system (MPS), delaying the immune system's fast elimination of it. Hydrophilicity and lipophilicity of the nanovesicle surface had the greatest effect on the phagocytic rate. Due to the strong interaction between the particle and opsonin, an adequate phagocytic impact is expected as the surface lipophilicity of the nanovesicles increases. Therefore, it is important to modify the nanoparticle surface to make it more hydrophilic to extend the in vivo circulation period of the nanoparticles. Polyethylene glycol (PEG), a hydrophilic polymer, is a potential solution to this problem (Xue et al., 2020). PEG is one of the most hydrophilic molecules, and is often used as an example of a stealth polymer. By creating an aqueous coating over the nanovesicles and preventing their renal clearance, PEGylation reduces their electrostatic charge. The PEG chains are also characterized by their flexibility and stretchability. To overcome the low penetration of drugs into the prostatic epithelium, reduce opsonization, and increase the time that nanoparticles spend in the bloodstream, in vivo biocompatible polymers such as polyethylene glycol (PEG) have been used to shield nanoparticle surfaces (Zhang et al., 2016). Therefore, a surface-attached ligand (monoclonal antibodies and their Fab fragments) has the potential to recognize and bind target tissues or cells with specificity (Torchilin, 1998). Several bacterial virulence factors and epitopes have been targeted by antibody treatments for infections, and much relevant research has been conducted on antibodies that target bacterial outer membrane proteins (OMP), particularly adhesion-related proteins (Ali et al., 2019; Jain et al., 2018; Le et al., 2018; Visan et al., 2018; Wang-Lin and Balthasar, 2018). Monoclonal antibodies (mAbs) are commonly used in medicine and research. The most common isotype is immunoglobulin G (IgG). IgGs are disulfide-bonded tetramers consisting of two identical heavy and light chains (Santamaria and de Groot, 2019). Antibodies were used to adjust to local pathological site stimuli, such as releasing an entrapped drug or specifically targeting cellular membranes under abnormal pH or temperature at disease sites (this property may be provided by surface-attached pH- or temperature-sensitive components), and to effectively target intracellular drug targets by penetrating cells without lysosomal degradation (O'Shaughnessy, 2003).

This study aimed to target the drug at the site of infection and overcome the poor penetration of antibiotics into the prostatic epithelium by fabricating a sustained-release transferosomal system adopting a factorial design accompanied by optimization and in vitro characterization of the selected formula. Transferosomes were used as carriers to encapsulate ciprofloxacin for the treatment of CBP, and the exterior of the nanomedicine was decorated with polyethylene glycol (PEG) to achieve prolonged circulation and active targeting in the body. Monoclonal antibodies have gained importance owing to their high specificity. Both in vitro and in vivo experiments demonstrated that the nanomedicine had good biocompatibility. In vitro, we used the transferosome as a carrier to encapsulate ciprofloxacin by testing different ratios of PC/Tween80/PEGylated agent and chloroform/methanol content on the entrapment efficiency (EE), release studies, particle size distribution, and zeta potential of the transferosome. In vivo experiments showed that ciprofloxacin-loaded transferosomes coupled with monoclonal antibodies accumulated in the prostatic lumen, and the released drugs significantly reduced inflammation of the prostate, which could significantly reduce the expression of the inflammatory marker (IL-1 β). It is expected that the encapsulation technique coupled with monoclonal antibody is the best preparation condition for improving the stability of ciprofloxacin, increasing penetration, reducing inflammation, and targeting the drug to the site of infection.

2. Materials and Methods

2.1. Reagent

Ciprofloxacin was a generous gift from Pharco Pharmaceutical Industries, Egypt, PEG-6-Stearate (molecular weight 548.79300) and Tween 80 were purchased from Sigma-Aldrich, USA. Soybean Lecithin

phosphatidylcholine (PC) was purchased from Lipoid GmbH, Germany, Enterobacteriaceae Monoclonal Antibody was obtained from San Diego, California, United States, and Rat IL-1 β Interleukin 1 Beta ELISA KIT was purchased from Elabscience, United States All other reagents were commercially available and of analytical grade.

2.2. Preparation of Transferosomes

Ciprofloxacin-loaded transferosomes were prepared using reverse-phase evaporation (Szoka and Papahadjopoulos, 1978). The lipid moiety (300 mg), including phosphatidylcholine (PC) and Tween 80, was weighed into a round-bottom flask and dissolved in a chloroform/methanol mixture (1:2 v/v). Organic solvents were evaporated under vacuum using a rotary evaporator (Buchi R-110 Rotavapor, Switzerland) at 40 °C to form a thin lipid film on the inner surface of the flask. The lipid film was re-dissolved in 10 mL of ether, followed by the addition of a drug solution (100 mg) in 10 mL of acetone and 10 mL of phosphate-buffered saline (PBS, pH 7.4). The mixture was then placed in a rotary evaporator to remove organic solvent. The transferosomes were allowed to equilibrate at room temperature and the transferosomal suspension was adjusted to a final volume of 10 mL with PBS. The suspensions were stored overnight in a refrigerator.

PEGylated transferosomes were prepared by adding 50 mg of PEG-6-stearate to the optimal transferosomal formulation.

2.3. Determination of Ciprofloxacin Entrapment Efficiency in Transferosomes

To determine the encapsulation efficiency (EE) of the transferosomes, a known quantity of transferosomes was centrifuged at 10,000 rpm for 30 min at 4 °C using a Beckman Coulter Inc. centrifuge (Fullerton, CA). The separated transferosomes were sonicated in methanol for 15 min to disrupt the vesicles and release encapsulated ciprofloxacin. The ciprofloxacin concentration in methanol was determined spectrophotometrically at 273 nm using a Shimadzu UV-1601 PC spectrophotometer (Japan). The entrapment efficiency (EE percent) was calculated as follows (Hosny, 2010).

$$EE\% = [Me/Mt] \times 100$$

Where Me and Mt. represent the amounts of encapsulated ciprofloxacin and total ciprofloxacin, respectively. The EE percentage was determined to evaluate the effect of PC/Tween 80 M ratios on the EE percentage using different molar ratios of PC/Tween 80 (5:1, 5:2, 5:3, 5:4, and 5:5) with constant ciprofloxacin content. EE% was also used to study the effect of PEGylated lipids in the selected transferosome formula.

2.4. Morphology and size Analysis of Transferosome

The physical morphology of samples of ciprofloxacin-loaded transferosomes composed of PC/Tween 80 in a molar ratio of 5:5 and ciprofloxacin-loaded transferosomes PEGylated PC/Tween 80/PEGylated agent in a molar ratio of 5:5:1 coupled with an antibody formula was examined using a transmission electron microscope (ZEISS, EM 10, Germany). To allow some of the transferosome particles to stick to the collodion, a drop of transferosome dispersion sample was placed on a 300-mesh collodion copper grid on paraffin and allowed to sit for 10 min. Excess dispersion was eliminated and a drop of 2% uranyl acetate solution was administered for two minutes. After the extraction of the remaining solution, the sample was air-dried before being measured under a transmission electron microscope. Laser diffraction particle-size analysis was performed to determine the mean particle size (Malvern Instruments Ltd., Malvern, UK).

2.5. In Vitro Drug Release and Release kinetics Studies

The in vitro release of ciprofloxacin from transferosomes was quantified using a dialysis technique. A Spectra/Pore® dialysis membrane was used for dialysis (12,000–14,000 molecular weight cutoff). This membrane ensures pharmaceutical penetration, while maintaining liposomal forms (El-Samaligy et al., 2006).

The ciprofloxacin transferosomal suspension (3 mg) was dispersed in 1 ml of PBS (pH 7.4) in a measuring cylinder with a length of 8 cm and a diameter of 2.5 cm. This cylinder was attached to a presoaked dialysis membrane prior to the addition of the transferosomal suspension, and it was placed in a dissolving flask filled with 75 ml of PBS (pH 7.4) and maintained at 37 °C in the USP dissolution tester (Pharma test, Hainburg, Germany). The glass cylinder was turned so that it rotated continuously (75 rpm). The release medium (4 ml) was removed at predefined intervals (0.5, 1, 1.5, 2, 3, 4, 6, 8, and 10 h) and spectrophotometrically measured for drug loading at 273 nm. In vitro release kinetics data from in vitro permeation studies were fitted to different kinetic models to study release kinetics. These models included Higuchi's zero-order model, which calculated the cumulative percent drug permeated vs. time, the cumulative percent drug permeated vs. square root of time, and first order as the log cumulative percentage of drug remaining vs. time.

2.6. Antibody Tagging to PEGylated Transferosomes

Periodate was used to oxidize the vesicles, and was added along with an equivalent volume of isotonic buffered solution. NaCl was added to periodate at concentrations below 60 mM. Normally, oxidation is allowed to continue for 30 min in the dark. The vesicles were subsequently separated from the periodate on a 1.5 10 cm Sephadex G-75 column that had been equilibrated in 20 mM borate and 120 mM NaCl (pH 8.4). As periodate oxidized Sephadex, the column was thrown away after usage (Heath et al., 1981).

Oxidized vesicles in 1 ml of 5–10 mol total lipid and 25 mg of Enterobacteriaceae Monoclonal Antibody IgG in 1 ml of 20 mM borate and 120 mM NaCl were combined for coupling with NaBH₄ (pH 8.4). After adding 0.2 M NaOH to the mixture to get the pH up to 9.5, the mixture was incubated for 2 h at 25 °C before NaBH₄ was added at a final concentration of 0.3 mg/ml and another hour at 25 °C. The mixture was then dissolved overnight in distilled water overnight (Heath et al., 1981).

2.7. Stability Studies

The aggregation propensity and drug leakage from the prepared vesicles were assessed during storage to determine their physical stability. Transferosomal vesicles were stored in transparent vials sealed with plastic caps (10 mL capacity) at 4 ± 1 °C, 25 ± 1 °C (ambient temperature), and 37 ± 1 °C (physiological temperature) for a period of 3 months. The vesicle size and entrapment efficiency (EE) were measured to evaluate the physical stability of the prepared vesicles throughout the study. At predetermined intervals, 2 mL samples were withdrawn from each transferosomal formulation. The vesicle size and EE of the vesicles were determined as previously described. Visual observation was used to assess the physical appearance of the vesicles for sedimentation. (Muppidi et al., 2012).

2.8. Animals

Adult male Wistar rats (Raypa tech, Cairo, Egypt) weighing 250–350 g were obtained. The Beni-Suef University animal ethical committee criteria and the Helsinki procedures were implemented in this investigation, and approval was obtained before the experiment started (approval code: FVM-BSU REC with approval number 05072020. and ensured that all animals were handled, weighed, and treated ethically in

accordance with the guidelines approved by the Institutional Animal Care and Use Committee at the Faculty of Veterinary Medicine at Beni-Suef University in Egypt. The rats were kept in plastic cages with wood chip bedding in climate-controlled rooms. (22 ± 2 °C) and humidity (40–60%), with food and water available. For two weeks before the experiment, animals were given full access to food and water and were allowed to acclimatize to their new environment.

2.9. Experimental groups

A total of twenty-five adult male Wistar rats were divided into 5 different groups of 5 rats each. 1) the normal group (G1), 2) the control group (G2) was given 500 μ L of sterility phosphate buffer saline, and groups 3,4, and 5 were exposed to injection of the 200 μ L *Enterobacter cloacae* strains suspension. After seven days of injecting bacteria, group 4 (G4) was treated with Cipro 5PEG, group 5 (G5) with Cipro 5PEG antibody tagged for 14 days and group 3 (G3) left a control positive.

2.10. Drug

Ciprofloxacin was given orally to rats in the treatment groups (G4 and G5), In order to allow the comparison of pharmacokinetic data, the oral formulations were given at a constant dose level of 3.5 mg/kg body weight/d which is comparable to the 500 mg/kg/d clinical therapeutic dose for humans determined according to the Paget and Barnes formula (Elsenosy et al., 2020; Paget and Barnes, 1964). To deliver the drug orally to rats by oral gavage, the drug was dissolved in 2 ml of distilled water.

2.11. Chronic Bacterial Prostatitis-Inducing Bacterial Pathogen

In our previously published article, we isolated and identified bacterial pathogens from the prostate secretion of ten patients diagnosed with chronic bacterial prostatitis at Kasr Al Ainy Hospital in Cairo, Egypt (DOI:10.21203/rs.3.rs-1,993,189/v1). *Enterobacter cloacae* strain MAG-06 (accession number, OK087614) was chosen to be the infective bacterium for Wistar rats to induce CBP as it recorded multiple drug resistance against three (Cefaclor, Azithromycin, and Aztreonam) out of seven tested antibiotics. To prepare the *Enterobacter cloacae* suspension, it was cultivated overnight in tryptic soy broth (TSB) at 37 °C. The cells were spun, washed three times, and resuspended in physiological saline at a concentration of 10^8 cells per milliliter.

2.12. Bacterial Prostatitis Model

For the injection of 200 μ L of *Enterobacter cloacae* strain suspension into the prostate, the sexual area of rats ($n = 25$) was anaesthetized with ether and catheterized with a 2.5 cm lubricated sterile polyethylene tube length after cleaning with 70% alcohol. The needle was connected to an insulin syringe, and 200 μ L of bacteria was injected. Anesthesia was maintained for 1 h to prevent urinary leaks.

2.13. Histopathological Analyses

All prostate tissues were taken from untreated and treated *Enterobacter*-infected animals, and they were all regularly processed through graduated alcohol concentrations and fixed in paraffin blocks. Five-micron pieces were cut, deparaffinized, and rehydrated in ethanol at progressively higher concentrations. After being rinsed with deionized water for 15 s, the tissues were stained with hematoxylin for 4 min and

dehydrated the samples for <5 s using 70% ethanol first, then 95% ethanol. For two minutes, eosin was used. After staining, samples were dried out in ethanol in increasing concentrations (95% ethanol for 5 s, 100% ethanol for 5 s, and then 100% ethanol for 5 s) and then cleaned in xylene (twice for <1 min each and once for 2 min) (Elkawahji et al., 2009).

2.14. Levels of Secretory Cytokines

The serum was separated from the blood for 15 min at a speed of 3500 rpm. The levels of IL-8, IL-1 β and TNF- α in serum were quantified by analysis kits (Elabscience, United States).

2.15. Statistical Method and Data Analysis

Statistical investigation All results were presented as mean \pm SEM. When data are normally distributed and sample variances are equal, one-way analysis of variance (ANOVA) is used, followed by post-hoc analysis and least significant difference (LSD) for intergroup comparison. P values of $P > 0.05$, $P > 0.05$, and $P > 0.001$ were regarded as non-significant, significant, and very significant, respectively.

3. Results and Discussion

3.1. Vesicle Size and Zeta Potential

The formulation of transfersomes was done by three dependent variables: phospholipid to surfactant ratio Soybean Lecithin phosphatidylcholine (PC), type of surfactant Tween 80 non-ionic edge activator (EA), and a solvent chloroform/methanol mixture, Fang et al. performed a further investigation into the effect of composition (Fang et al., 2001). Soy phosphatidylcholine has a role in creating the lipid bilayer that can be a mixture of lipids, which are vesicle-forming (Jiang et al., 2018; Rahmi and Pangesti, 2018). Soya phosphatidylcholine contains a lot of components and the most important it is phosphatidylcholine, phosphatidylethanolamine, phosphatidylinositol, and unsaturated fatty acid, and the existence of unsaturated fatty acids improve and facilitate the penetration of bioactive compounds (Valenta et al., 2000) and it has a long alkyl chain produced hard bilayers which has a low permeability For encapsulated compounds (Talsma and Crommelin, 1993). Tween 80 was found a better edge activator in transfersome preparations which is a biocompatible bilayer-softening compound that increases the vesicles' bilayer flexibility, produces formulations with smaller particle sizes with a higher drug entrapment efficiency, produces prolonged drug release (Khan et al., 2015), and improves the permeability (Ascenso et al., 2015; Jain and Kumar, 2017; Jiang et al., 2018; Kotla et al., 2017; Rajan et al., 2011). Transfersomes were prepared with different ratios of Tween 80 to determine the best formula of transfersome as shown in Table 1.

The vesicle size distribution curve was unimodal in shape Fig. 2. The prepared transfersomes revealed vesicles with sizes in the range 202.59 ± 1.46 nm to 94.69 ± 1.71 nm Table 1. Among the five formulations, Cipro 5 (PC/Tween 80, 5:5) showed the smallest size 94.69 ± 1.71 nm and thus was chosen for further studies. It was noticed that with increasing Tween 80 concentration, the vesicle size of drug-loaded transfersomes decreased. Due to the high concentration of Tween 80 and the low concentration of phospholipid available for vesicle formation. This results from the creation of micelles instead of vesicles, which are smaller in size. and it also Tween 80 has a difference in hydrophilic-lipophile balance (HLB) values of the surfactant which has a high HLB value and a higher interaction with the aqueous phase which leads to a

Table 1
Physical characteristics of the formulated ciprofloxacin-loaded transfersomes.

Formula	lipid	SA	PEG	Ratio	Size (nm)	Zeta potential (mV)	EE (%)
Cipro 1	PC	Tween 80		5:1	153 ± 1.55 ^a	-39.15 ± 1.79 ^c	85.5500 ± 1.34 ^d
Cipro 2	PC	Tween 80		5:2	125.42 ± 1.15 ^b	-35.35 ± 1.03 ^c	82.05 ± 2.47 ^{cd}
Cipro 3	PC	Tween 80		5:3	120.4 ± 1.48 ^c	-22.91 ± 2 ^b	79.27 ± 2.15 ^{bc}
Cipro 4	PC	Tween 80		5:4	111.42 ± 1.52 ^d	-20.21 ± 1.73 ^b	74.95 ± 1.2 ^{ab}
Cipro 5	PC	Tween 80		5:5	94.69 ± 1.71 ^e	-13.12 ± 1.81 ^a	71.05 ± 1.76 ^a
Cipro 5PEG	PC	Tween 80	PEG	3:3:1	202.59 ± 1.46 ^f	-49.38 ± 1.0 ^d	80.05 ± 1.62 ^c
AB-Cipro 5PEG	PC	Tween 80	PEG	3:3:1	223.36 ± 2.59 ^f	-50.35 ± 3.2 ^d	81.33 ± 2.98 ^c

Ratio = lipids: surfactant: PEG. (w.w.w) PC: Soy phosphatidylcholine, SA: surfactant (Tween 80), PEG: polyethylene glycol. Cipro 1: ciprofloxacin -loaded transfersomes, Cipro 5PEG: ciprofloxacin-loaded transfersomes PEGylated (PC/Tween80/PEG6 stearate, 3:3:1). EE: Entrapment efficiency. Amount of drug: 3 mg/mL. Results are presented as the mean ± SD ($n = 3$); means carrying different superscript letter(s) within the same column were considered significantly different at $P < 0.05$ determined by one-way ANOVA.

lower vesicle size (Jain et al., 2003; Khan et al., 2015). When the formulation was made at the ratio of Cipro 5 (PC/Tween 80, 5:5) the smallest average size was 94.69 ± 1.71 nm. The formulation of Cipro 1 (PC/Tween 80, 5:1) had a vesicle size of 153 ± 1.55 nm was a significant difference ($P < 0.05$) compared with an increased concentration of Tween 80. Furthermore, our results agree with the findings of Ahad et al., who found that an increase in the PC/Tween 80 ratio resulted in a reduction in the particle size of transfersome containing bile salt (Ahad et al., 2018). It was shown that PEGylated transfersome with a ratio of (PC/Tween 80/PEG 3:3:1) was significantly larger in size than non-PEGylated transfersome ($P < 0.05$) with a ratio of (PC/Tween 80, 5:5) (Table 1) demonstrating the potential positioning of the PEG moieties on the loaded nanostructured lipid carrier surface (Garcia-Fuentes et al., 2003). Furthermore adding PEG-6-stearate led to a remarkable was significantly ($P < 0.05$) increase in the vesicle size (≈ 200 nm) compared to non-PEGylated (93.6 nm) despite having the same ratio of (PC/Tween 80, 5:5). This could be attributed to the rigidity of the PEGylated lipid, which leads to rapid assembly of the vesicles and resistance to size reduction.

Zeta potential is a vital surface characterization technique used in identifying the surface charge and potential stability of nanoparticulate. For colloidal dispersion stability, an absolute large negative or positive zeta potential value is typically necessary because electrostatic repulsion prevents the accumulation of particles with the same charges and for assessing the effects of different materials, which include membrane stabilizers and EAs, impacted the way nanoparticles formed (Hassanpour et al., 2020; Manjunath et al., 2005; Nguyen et al., 2021). The zeta potentials of formulations were in the range of -13.2 ± 3.02 to -39.2 ± 6.25 mV (Table 1) which agrees with the study of Amnuait, Thanaporn, et al. that all transfersome formulations had strong negative charge zeta potentials. The increasing zeta potential of transfersomes may be attributable to increasing the ratio of tween 80 over the negatively charged lecithin in 7.4 pH (Khan et al., 2022). A zeta potential greater than ± 30 mV indicates that the formulations are stable because the repulsive force of the same charge can prevent particle aggregation (Amnuait et al., 2018; Zhao et al., 2015). Since Tween 80 is a nonionic surfactant, transfersomes containing it as an edge activator may have surfaces that are negatively charged as a result of the partial hydrolysis of Tween80's polyethylene oxide head groups, or $(\text{CH}_2\text{-CH}_2\text{-O})_n$ (Zeb et al., 2016). Lecithin, an amphoteric lipophilic surfactant, was present, which allowed the predominant charge of the particles to be negative. PEG is a biodegradable polymer that has been used in different drug delivery systems because of its superior biocompatibility and lack of toxicity (Sinha et al., 2013). In (Table 1) Incorporating PEG-6-stearate led to a significantly decrease ($P < 0.05$) in zeta potential compared with non-PEGylated due to the stearate groups (Faddeel et al., 2020;

Pena-Rodríguez et al., 2020). PEG cipro5 was -49.38 ± 1.0 mV, Due to PEG having a hydroxyl end which was ionized at pH 7.4. Zeta potential is more negatively charged. Moreover, PEG immobilized on the transfersome surface which is on the negative side (Abdelbary et al., 2019; Davarpanah et al., 2018; Ehi-Eromosele et al., 2016). This negative zeta potential has also been established in previous studies that synthesized various PEG nanocarriers and particular coating nanoparticles with PEG-6 stearate can reduce the zeta potential, our findings are the same as the results reported by Rostami, Elham, et al. (Cruz et al., 2011; Davarpanah et al., 2018; Kashanian and Rostami, 2014; Naik et al., 2010).

3.2. Entrapment Efficiency (EE)

Entrapment efficiency is the percentage of the drug's total concentration in the vesicles that were integrated into the transfersomes. The prepared transfersomes showed an entrapment effectiveness in the range of $71.05 \pm 1.76\%$ to $85.5500 \pm 1.34\%$. It was noticed that as we increased the Tween 80 ratio in formulation Cipro 5 (PC/Tween 80, 5:5) the entrapment efficiency was found to be decreased significantly ($P < 0.05$) $71.05 \pm 1.76\%$ in comparison to the formulation Cipro 1 (PC/Tween 80, 5:1) $85.5500 \pm 1.34\%$. According to researchers, this may be caused by the existence of mixed micelles with vesicles or pore formation within the vesicles at higher surfactant concentrations (Edwards and Almgren, 1990). These findings could be attributed to the increased fluidity of the vesicle wall. (Table 1) show how the Tween 80 ratio affects the effectiveness of the trapping of ciprofloxacin. The findings of other researchers agree with the decrease in entrapment efficiency that occurs when the amount of Tween 80 in the formulation is increased (Khan et al., 2015). In the formulation, the entrapment efficiency significantly declined. Lower entrapment efficiency in the formulation. The percent encapsulation efficiency (%EE) of PEGylated 5 ciprofloxacin-loaded transfersomes was meticulously calculated to obtain the remarkable value of $80.05 \pm 1.62\%$. A comprehensive investigation showed the importance of PEGylated drug formula in determining the efficacy of drug entrapment within these nanoparticles and precisely encapsulating ciprofloxacin, showing the quality and perfection of this advanced method. Incorporating PEGylated lipid into the chosen transfersome formula led to an increase in rigidity of the vesicles and was significantly decreased leaking ($P < 0.05$) in Cipro 5PEG formula ($80.05 \pm 1.62\%$) in comparison to un-PEGylated Cipro 5 ($71.05 \pm 1.76\%$) as was proven from the tabulated data. Linking antibodies to PEGylated vesicles led to an increase in vesicle size, zeta potential and EE %. Antibodies linked to the terminal PEG chains from the vesicles increases the rigidity of the formed vesicles and hence retain more drug inside the vesicles.

3.3. In Vitro drug Release studies and kinetics

The most important aspect of the reasonable design of a drug release system is the kinetics of drug release from a nanocarrier formulation since it strongly impacts the efficacy and release of free drug in vivo (Hua, 2014). To minimize frequent administration and foster better patient compliance, the ideal formulation should permit a prolonged medication release (Madan et al., 2014). Cip-loaded transfersomes and cipro 5PEG were compared in the release medium of phosphate buffered saline (PBS, pH 7.4) which approached physiological pH (Chen et al., 2020) (Fig. 1). The drug release profiles in vitro for a total amount of free ciprofloxacin of 3 mg suspension dispersed in 1 ml of PBS (pH 7.4). The drug release from nanoparticles was assessed by dialysis membrane. The percent release of ciprofloxacin increased with an increase of Tween 80 proportion (as illustrated in Fig. 3 and Table 1). This could be attributed to the increased fluidity and leakage of vesicles with increased Tween 80 proportion in the vesicles (El-Samaligy et al., 2006). So the cipro 5 with PC: Tween 80 5:5 showed $89 \pm 8.1\%$ drug release compared with the cipro 1 with PC/Tween 80 1:5 showed $63 \pm 5.8\%$ drug release. Incorporating PEGylated lipid into the vesicles led to a slower drug release ($80 \pm 3.1\%$) which came with the results regarding EE% and size due to the increased vesicle rigidity and decreased leaking of drug from transfersome may be associated with the presence of a PEG corona on the surface of the transfersome, which reduced the diffusion of drug from the transfersome interior because of the rapid movement of the

PEG hydrophilic chain (Abdel Fadeel et al., 2020; Ramana et al., 2012). The linkage of antibodies to liposomes can enhance the stability of the liposomes and prevent premature drug release (Ansell et al., 2000). Covalent linkage of antibodies to liposomes can result in a high-density array of antibodies that is stable in various conditions (Bale et al., 2017).

Additionally, we studied drug-release kinetics, which is an essential field of pharmaceutical research that includes studying the time-dependent behaviour of drug post administrations. Release kinetics of the formulated transfersomes are shown in Table 2. The formulations of cipro 5 and cipro 5PEG were best fitted for the first order equation as the formulation coefficient of correlation values predominates over zero-order and Higuchi Model kinetics. First-order release from transfersomes refers to a release mechanism where the rate of drug release is proportional to the concentration of the drug remaining in the transfersomes. This means that the release rate decreases exponentially over time as illustrated in Table 2. The first-order release kinetics can be described by a mathematical model that takes into account factors such as the composition of the transfersomes and the conditions of release (Jain and Jain, 2016). The release rate constant in the first-order model is influenced by various parameters, including the solubility of the drug, the permeability constant of the drug in the transfersomes, and the size of the transfersomes (Guy et al., 2011). The release rate of transfersomes can also be affected by the length of the acyl chain of the drug, with longer chain lengths resulting in slower release rates (Okada et al., 1991). Moreover, this might be owing to the transfersome's surface

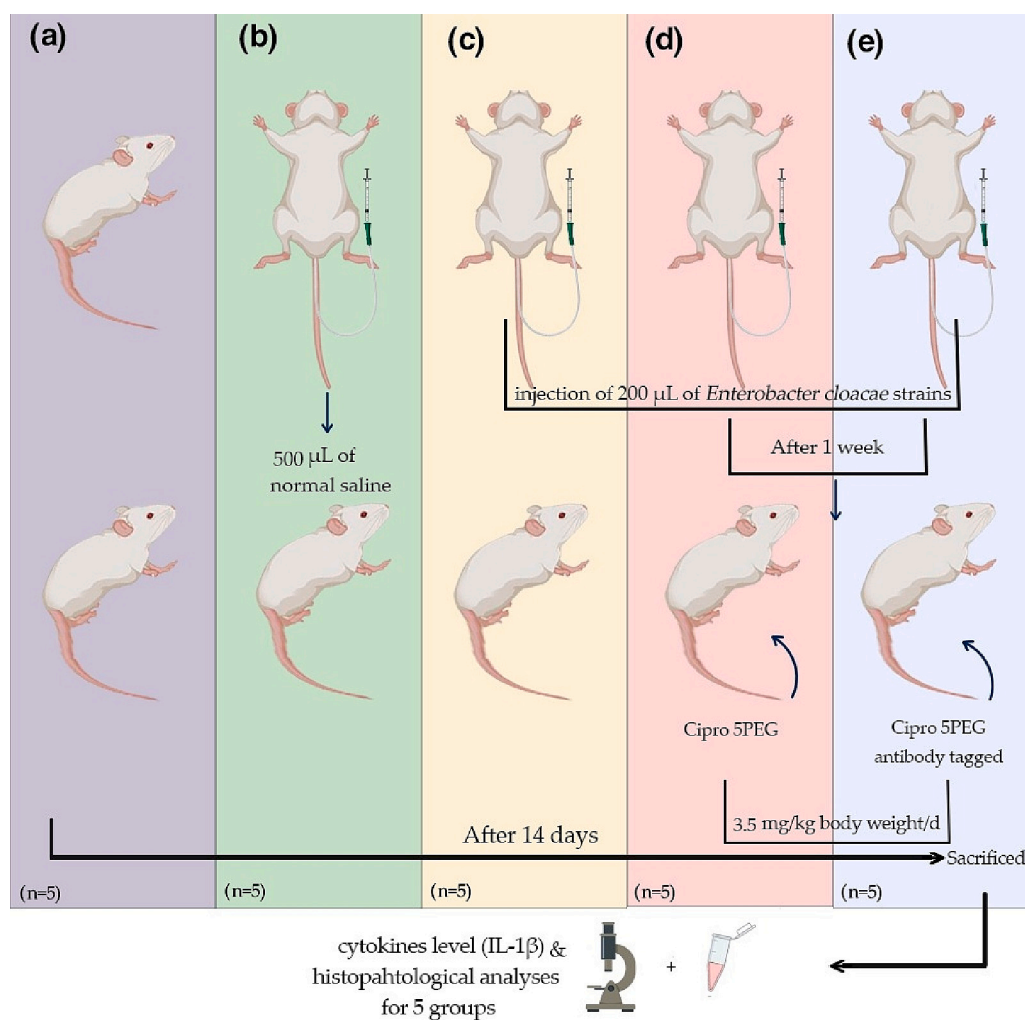


Fig. 1. An overview of animal models and experimental design. (a), (G1) normal (b), (G2) control (c), (G3) control positive (d), (G4) Cipro 5PEG and (e) (G5) Cipro 5PEG antibody tagged.

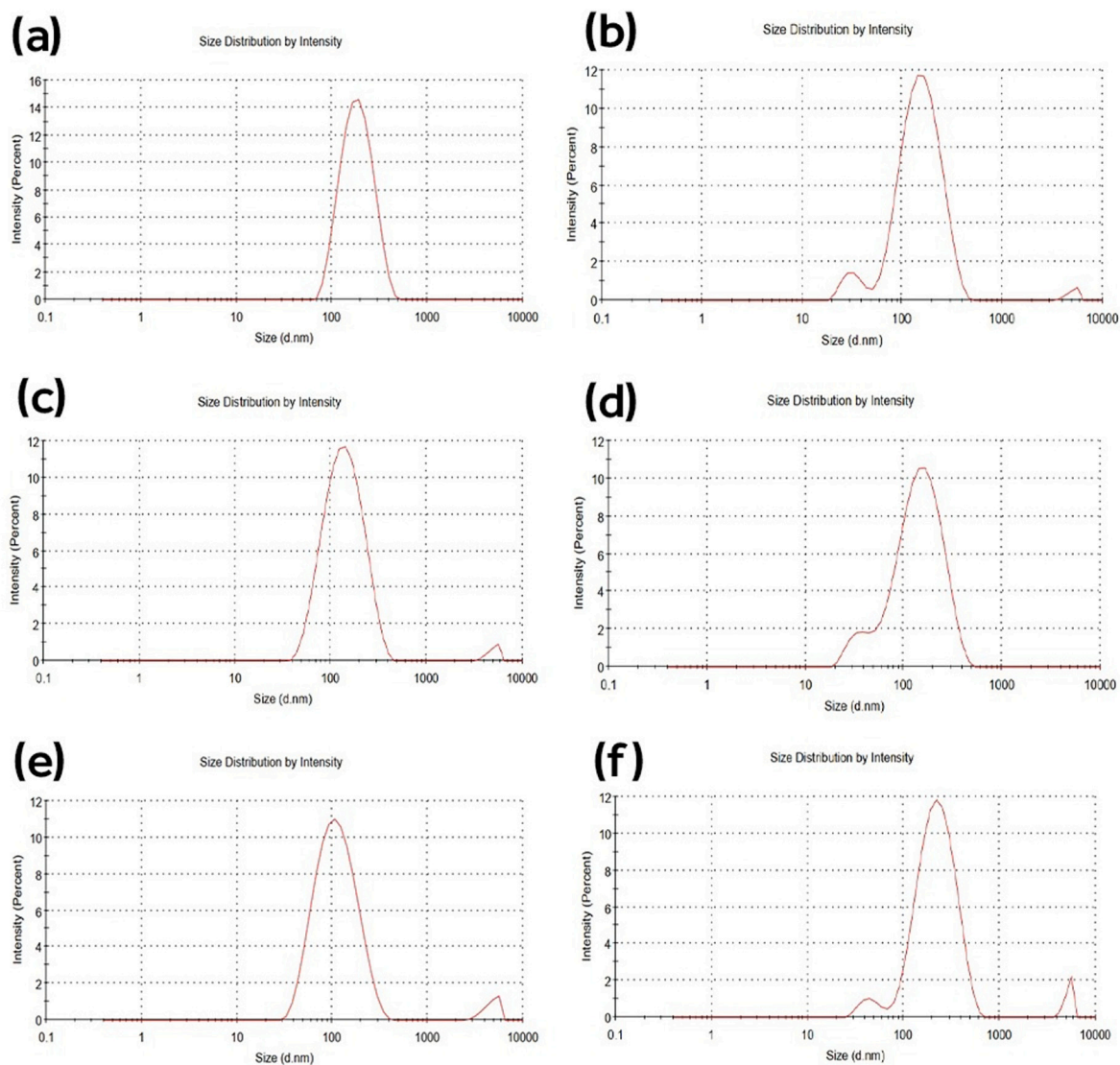


Fig. 2. Ciprofloxacin-loaded transfosomal size distribution (a) Cipro 1, (b) Cipro 2, (c) Cipro 3, (d) Cipro4, (e) Cipro 5 and (f) Cipro 5 PEG.

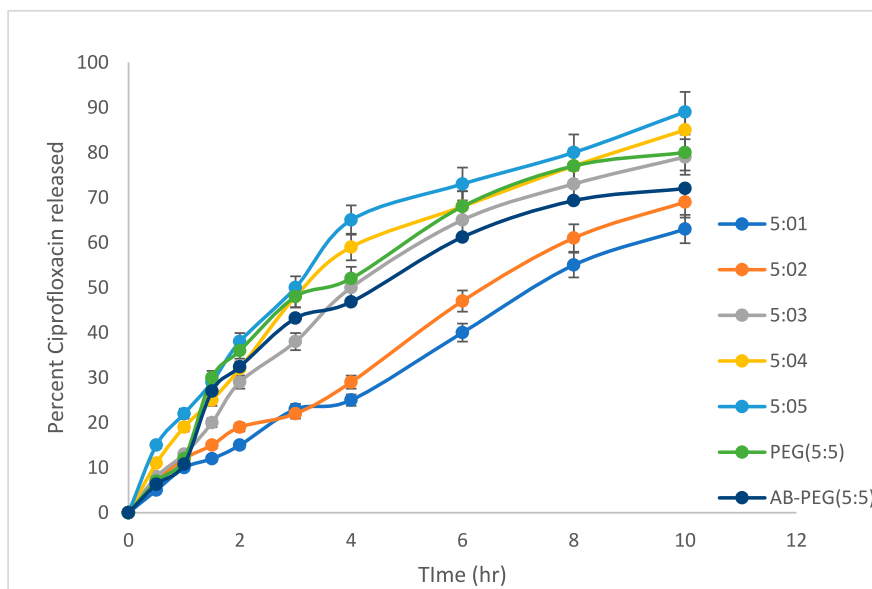


Fig. 3. In vitro drug release profile of formulated ciprofloxacin-loaded transfosomes and PEGylated 5 ciprofloxacin loaded transfosomal suspension in comparison to its solution (mean \pm SD, $n = 6$).

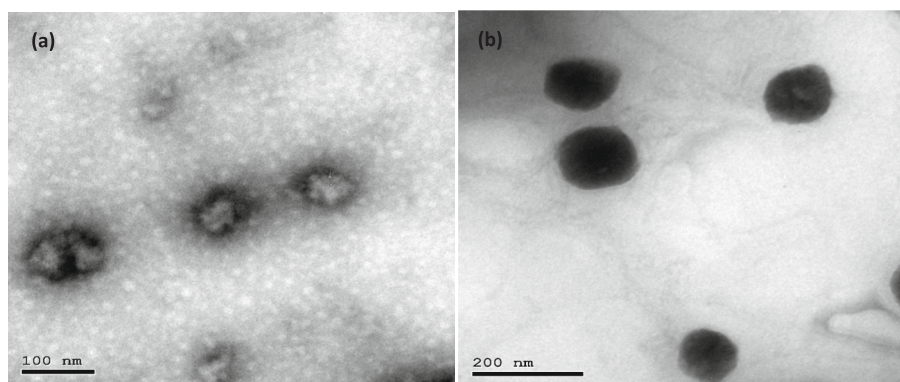


Fig. 4. TEM image of formula Cipro 5 (a) and (b) Cipro 5 PEGylated Cip-loaded transferosome (Cipro 5PEG) coupled with IgG antibody.

being covered in PEG. It is established that PEG can sterically hinder vesicles by forming a hydrolayer on the surface of vesicles. This slows down the rate of phagocytosis and degeneration by preventing vesicles from coming into contact with opsonin and proteases (Li et al., 2017).

3.4. Vesicle Morphology

Transmission electron microscope images of formula Cipro 5 (5:5) PC/Tween 80 and formula Cipro 5PEG decorated with IgG antibodies are shown in Fig. 4. Both images showed well-organized double-layered vesicles. Images of Cipro 5PEG showed a distinct layer which was supposed to be the corona layer with hooked antibodies. PEGylated lipids are able to improve the stability of the produced nanoparticles and prevent agglomeration since the synthesis of polymeric-coated nanoparticles has advantages for drug delivery because PEG may form an

aqueous layer on the nanoparticle surface, which hinders PEGylated 5 ciprofloxacin loaded transferosomal aggregation due to steric hindrance (Garcia-Fuentes et al., 2004; Kamel et al., 2019; Shehata et al., 2016). Fig. 4a shows aggregation due to a lack of PEGylation, in contrast to Fig. 4b, where the vesicles separate because of the PEGylated agent.

3.5. In Vivo Therapeutic Efficacy of Cipro 5PEG Antibody Tagged Formula on Histopathology in a CBP Model

The prostate's peripheral, which is the most typical site of tumorigenesis, exhibits a high incidence of inflammatory alterations, according to histopathological examinations of prostates (McNeal, 1988). Moreover, males with chronic prostatitis exhibit a significant prevalence of bacterial species that have been inconclusively discovered in the prostate, according to molecular epidemiology investigations (Hochreiter et al., 2000). To investigate the connections between bacterial infection and inflammation, we developed an experimental animal model of bacterial prostatitis. In this investigation, all the male animals—known to be more susceptible to infection—developed both acute and severe forms of chronic bacterial prostatitis. A localized acute inflammation within the prostate as well as persistent prostatic inflammation were also brought on by bacterial infection. What was most notable was the atypical hyperplasia of the prostatic glandular epithelium, which was connected to an increase in epithelial cell layers, cytological atypia, and dysplastic changes in glandular architecture marked with green arrows. Control animals, on the other hand, never experienced prostate irritation or infection. These outcomes align with what was shown in rats (George et al., 1981; Reznik et al., 1981). As we show in Fig. 5 (a, b), normal and control groups the prostatic glands are intact without atrophy or destruction, intact glandular epithelium and abundant secretion in the glandular space marked with purple arrows. In bacterial infection (G3), the prostatic glands are markedly deformed and destroyed, the glandular epithelium is exfoliated and necrotic, and the secretions in the gland cavity are markedly reduced with (blue arrows) Fig. 4c. There is significant inflammatory cellular infiltration in the stroma. (H & E). In the Cipro 5PEG group (G4), the prostatic glands are slightly deformed and the secretions in the glands are reduced Figure in Fig. 4d. Significant inflammatory cellular infiltration is observed. In Fig. 4e, group (G5) was injected with a Cipro 5PEG-tagged antibody, which made the drug more effective than G4 because the drug was tagged with an Enterobacteriaceae monoclonal antibody that was selective for the bacterial infection strain *Enterobacter cloacae*. As expected, the inflammatory cellular infiltrate in the stroma was reduced and the prostatic glands were more enhanced, which is intact and without atrophy or destruction. The development of multidrug-resistant bacteria, extended-spectrum beta-lactamase-producing bacteria, the construction of bacterial biofilms, and the change in bacterial etiology are all global concerns for antibacterial treatment that have given rise from all over the world (Xiong et al., 2020).

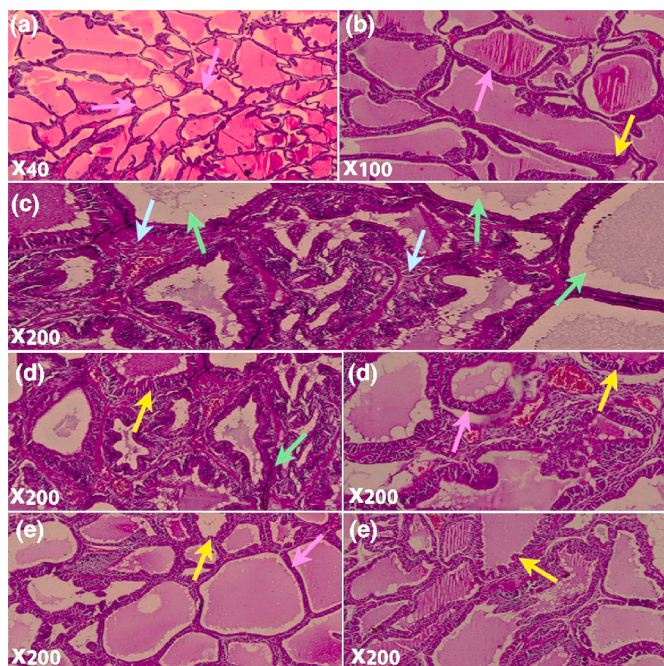


Fig. 5. H&E-stained sections of prostate tissues (a), normal (G1) are scanned at 40× magnification (b), control (G2) are scanned at 100× magnification (c), control positive (G3), (d), Cipro 5PEG (G4) are scanned at 200× magnification and (e) Cipro 5PEG antibody tagged (G5) are scanned at 200× magnification. Blue arrows indicate inflammatory cell infiltration, yellow arrows indicate Normal tall columnar epithelium, purple arrow indicate intact glandular epithelium and green arrows the presence of an atrophic gland. (For interpretation of the references to color in this figure legend, the reader is referred to the web version of this article.)

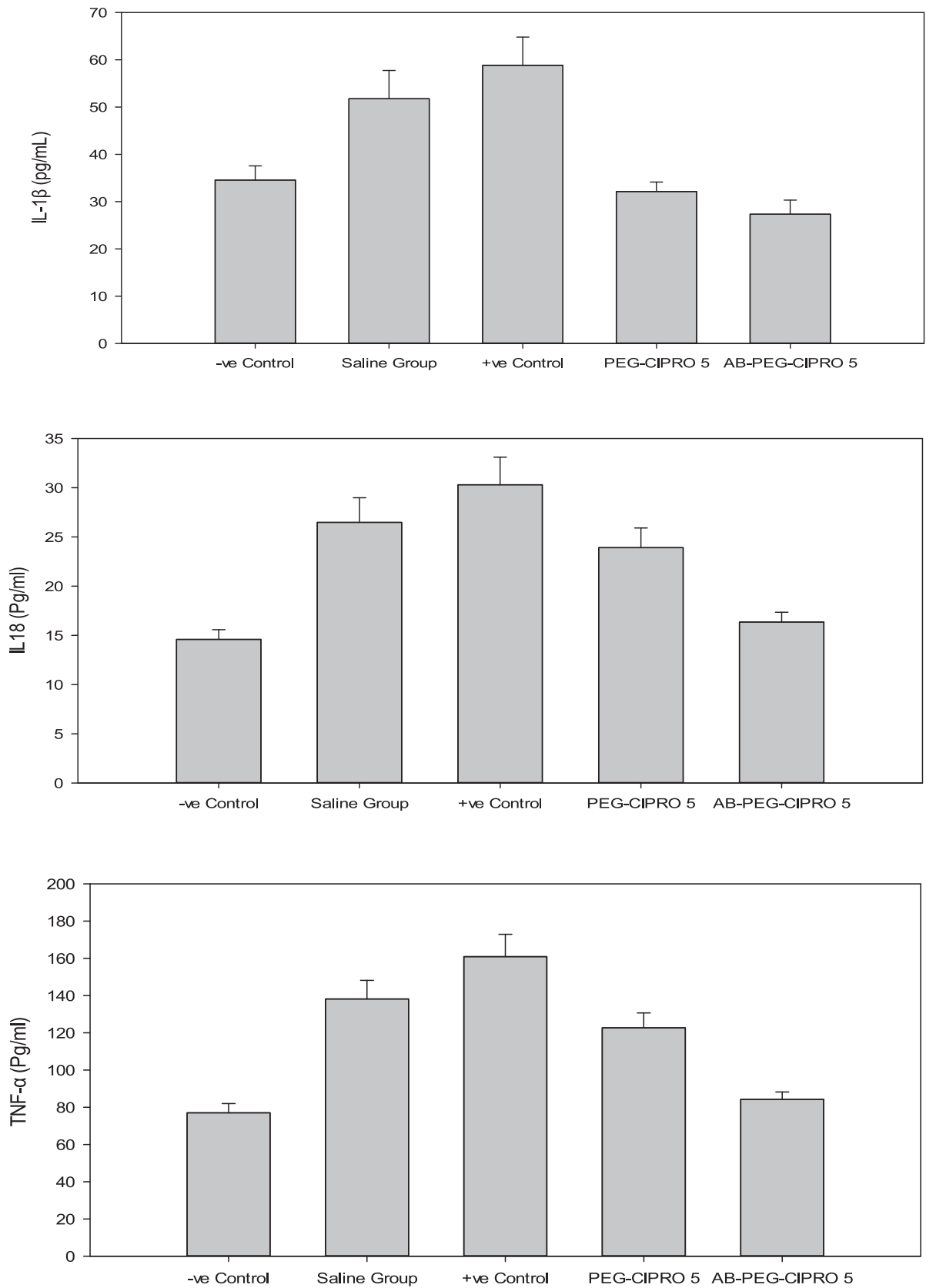


Fig. 6. The inhibiting proinflammatory mediators by Cip 5PEG antibody tagged treatment in a rat model of chronic bacterial prostatitis. Result represents the mean \pm SD ($n = 3$).

Table 2

Drug release kinetics of the formulated ciprofloxacin-loaded transfersomes.

Batch No.	Cipro 1	Cipro2	Cipro 3	Cipro 4	Cipro 5	Cipro 5 PEG	AB-Cipro 5 PEG
Model name	R2	R2	R2	R2	R2	R2	R2
Zero order	0.9662	0.9532	0.9936	0.9929	0.9852	0.9363	0.9465
First order	0.9753	0.9791	0.9938	0.9936	0.9886	0.9627	0.9981
Higuchi Model	0.9546	0.9701	0.9229	0.9391	0.9574	0.9118	0.9211

3.6. Effect of Transfersome Formula on Cytokines Levels

Some CBP symptoms may be associated with inflammation. Numerous clinical urologists have found elevated serum levels of IL-1 β in cases of chronic bacterial prostatitis, which are clinically used to assess prognostic biomarkers (Alexander et al., 1998; Nadler et al., 2000). To investigate the effect of transfersomes on cytokines, the level of IL-1 β in serum was measured. When compared to controls, CBP patients release more of the inflammatory protein IL-1 β as in Fig. 6 (Guo et al., 2012). As expected, significant elevation in the levels of IL-1 β was found in injected rats with bacteria (58.82 ± 3.79 pg/ml) versus the normal (27.33 ± 2.62 pg/ml) and treated rats with transfersomes (51.76 ± 5.39 pg/ml) ($P < 0.05$). Cipro 5PEG tagged antibody could effectively reduce proinflammatory cytokine expression in bacteria-infected cells. Transfersomes treatment maximally reduced the level of cytokine (IL-1 β) (34.56 ± 3.14 pg/ml) ($P < 0.05$) compared to other groups.

A clinical entity that occurs frequently is chronic bacterial prostatitis, which is still challenging to adequately control. Prostate tissue damage and hyperplasia brought on by inflammation through the production of inflammatory mediators released by many cell types are out of proportion to the painful symptoms (Atawia et al., 2014). Several studies have demonstrated the importance of the inflammatory response brought on by bacterial infection and the destruction of tissue or hyperplasia caused by the interactions of vital mediators, such as cytokines (Nickel et al., 2008). Many clinical urologists have observed elevated levels of IL-1 β and IL-8 in the serum from studies including men with chronic prostatitis. These levels are clinically used to assess predicting biomarkers (Alexander et al., 1998; Nadler et al., 2000).

Significant elevation in the levels of IL-8 was found in injected rats with bacteria (30.32 ± 2.79 pg/ml) versus the normal (14.58 ± 1.62 pg/ml) and treated rats with transfersomes (23.91 ± 2.39 pg/ml) ($P < 0.05$). Cipro 5PEG tagged antibody could effectively reduce proinflammatory cytokine expression in bacteria-infected cells. Transfersomes treatment maximally reduced the level of cytokine (IL-8) (16.35 ± 2.14 pg/ml) ($P < 0.05$) compared to other groups.

IL-8 is a chemokine that attracts neutrophils and mononuclear cells to inflammatory sites in prostate secretions, thereby making it one of the indicators used to evaluate men with chronic prostatitis. It is triggered by a variety of stimuli, including microbial and chemical stimuli as well as specific cytokines. It promotes inflammation and is involved in various conditions related to inflammation and increasing its value as a biomarker for prostate inflammation. According to Penna et al.'s study, IL-8 was significantly higher in CP patients than in controls. (Penna et al., 2007).

In accordance with other mediators, significant elevation in the levels of TNF- α was found in injected rats with bacteria (160.92 ± 3.79 pg/ml) versus the normal (76.97 ± 1.62 pg/ml) and treated rats with transfersomes (122.76 ± 8.39 pg/ml) ($P < 0.05$). Cipro 5PEG tagged antibody could effectively reduce proinflammatory cytokine expression in bacteria-infected cells. Transfersomes treatment maximally reduced the level of TNF- α (84.25 ± 5.14 pg/ml) ($P < 0.05$) compared to other groups.

TNF- α is another pro-inflammatory cytokine that is being expressed progressively in prostate tissue. It stimulates the production and release of several inflammatory markers by activating the NF- κ B pathway by causing I κ B to be phosphorylated. TNF- α is highly correlated with increased prostate volume in patients with chronic prostatitis, and it also

Table 3Effect on storage at different temperatures on EE% and vesicle size of the selected PEGylated transfersomes and the antibody tagged formula (mean \pm SD) $P < 0.05$.

Formula	EE%			Size (nm)		
Temperature	4 °C	25 °C	37 °C	4 °C	25 °C	37 °C
Cipro 5PEG	83 \pm 7.32	75 \pm 8.15	66 \pm 12.56	202.7 \pm 12.25	233 \pm 35.23	521 \pm 30.58
Cipro 5PEG antibody tagged	79 \pm 6.25	70 \pm 8.16	59 \pm 9.25	223.8 \pm 20.25	300 \pm 50.36	555 \pm 28.25

plays a role in the hyperalgesic effect in patients with chronic pelvic pain syndrome (Rahman et al., 2002).

Bacterial antibody-linked nanocarriers have potential benefits in the treatment of bacterial prostatitis. These nanocarriers can effectively deliver antimicrobial drugs to the target bacteria, such as *Staphylococcus aureus*, which is a commonly virulent human pathogen (Hu et al., 2022). The targeting nanoparticles preferentially bind to the bacteria and accumulate in the biofilm, enhancing the bactericidal activity against *S. aureus* in both planktonic and biofilm forms (Le et al., 2020). In addition, the use of nanocarriers can improve the biodistribution of antibiotics, leading to improved therapeutic efficacy (Liu et al., 2021). Furthermore, nanotechnology offers the possibility of developing targeted nanoparticle delivery strategies that can overcome the limitations of free drugs in penetrating the prostate epithelium and targeting inflammatory tissues (Cheng et al., 2019). By modifying the physicochemical properties of nanoparticles, such as size and surface ligands, their targeting effectiveness can be optimized (Kulkarni and Sonawane, 2017).

3.7. Stability Studies

The stability study results for the selected transfersosomal formulation are presented in Table 3. The EE% and vesicle size of transfersomes stored at 4 °C under refrigerated conditions did not exhibit significant changes ($P < 0.05$). However, transfersomes stored at higher temperatures showed significant changes ($P < 0.05$) in the measured parameters. A dramatic increase in vesicle size and drug leakage was observed at both room and physiological temperatures. Vesicles stored under refrigerated conditions were able to retain a higher percentage of the drug compared to those stored at elevated temperatures. By the end of the study, all vesicles stored at 4 °C were physically stable. No sedimentation or change in color was observed. The transfersomes stored at room temperature showed slight sedimentation, which could be easily redispersed upon shaking. At 37 °C, the color of the transfersosomal suspensions changed to pale yellow, and sediment formed that was not dispersible upon shaking.

4. Conclusion

Ciprofloxacin has been successfully incorporated into the transfersome using the reverse-phase evaporation technique. The obtained results confirmed that the PEGylated transfersome contained (PC/Tween 80/PEG, 3:3:1) had a high encapsulation efficiency, small particle size, negative charge in zeta size, and long-lasting drug in vitro release, which was better than un-PEGylated formula with the same ratios of PC and Tween 80. To provide more specificity to the site of

infection in CBP treatment, vesicles were coupled with the monoclonal antibody IgG. In this study, it was observed that a male rat model's persistent bacterial prostate inflammation is inhibited, which significantly reduced (IL-1 β , IL-8, and TNF- α) levels in serum and inflammations in the prostate tissues when compared to the control positive group. The drug did not inflame prostate tissues, according to a histological analysis. It has been shown that targeted delivery systems in therapy may deliver therapies selectively and lower treatment side effects. As a result, the development of a new monoclonal antibody coupled with nanoparticles as a targeted drug delivery approach to therapy is promising. Furthermore, the quality, effectiveness, and safety profile of drugs would significantly improve. The use of bacterial antibody-linked nanocarriers in the treatment of bacterial prostatitis can enhance drug delivery, improve therapeutic efficacy, and overcome treatment limitations.

Funding

This study was supported via funding from Prince Sattam Bin Abdulaziz University Project number (PSAU/2024/R/1445).

Institutional Review Board Statement

Not applicable.

Informed Consent Statement

Not applicable.

CRedit authorship contribution statement

Sahar I. Mohammad: Resources, Project administration, Methodology, Investigation. **Basmah Nasser Aldosari:** Funding acquisition, Formal analysis, Data curation, Conceptualization. **Magda M. Mehanni:** Writing – review & editing, Visualization, Validation, Supervision, Software. **Ahmed O. El-Gendy:** Writing – original draft, Supervision, Project administration, Methodology, Investigation. **Walaa G. Hozayen:** Visualization, Supervision, Resources, Project administration. **Obaid Afzal:** Visualization, Validation, Project administration, Investigation. **Randa Mohammed Zaki:** Funding acquisition, Formal analysis, Data curation, Conceptualization. **Ossama M. Sayed:** Writing – review & editing, Writing – original draft, Supervision, Software, Investigation.

Declaration of competing interest

The authors declare the following financial interests/personal relationships which may be considered as potential competing interests:

Randa mohammed zaki reports financial support was provided by Prince Sattam bin Abdulaziz University. If there are other authors, they declare that they have no known competing financial interests or personal relationships that could have appeared to influence the work reported in this paper.

Data Availability Statement

The data is contained in the manuscript.

References

- Abdel Fadeel, D.A., Kamel, R., Fadel, M., 2020. Pegylated lipid nanocarrier for enhancing photodynamic therapy of skin carcinoma using curcumin: in-vitro/in-vivo studies and histopathological examination. *Sci. Rep.* 10, 10435. <https://doi.org/10.1038/s41598-020-67349-z>.
- Abdelbary, A.A., Abd-Elsalam, W.H., Al-Mahallawi, A.M., 2019. Fabrication of levofloxacin polyethylene glycol decorated nanoliposomes for enhanced management of acute Otitis media: statistical optimization, trans-tympanic

- permeation and in vivo evaluation. *Int. J. Pharm.* 559, 201–209. <https://doi.org/10.1016/j.ijpharm.2019.01.037>.
- Ahad, A., Raish, M., Ahmad, A., Al-Jenoobi, F.I., Al-Mohizea, A.M., 2018. Eprosartan mesylate loaded bilosomes as potential nano-carriers against diabetic nephropathy in streptozotocin-induced diabetic rats. *Eur. J. Pharm. Sci.* 111, 409–417. <https://doi.org/10.1016/j.ejps.2017.10.012>.
- Alexander, R.B., Ponniah, S., Hasday, J., Hebel, J.R., 1998. Elevated levels of proinflammatory cytokines in the semen of patients with chronic prostatitis/chronic pelvic pain syndrome. *Urology* 52, 744–749. [https://doi.org/10.1016/S0090-4295\(98\)00390-2](https://doi.org/10.1016/S0090-4295(98)00390-2).
- Ali, S.O., Yu, X.Q., Robbie, G.J., Wu, Y., Shoemaker, K., Yu, L., DiGiandomenico, A., Keller, A.E., Anude, C., Hernandez-Illas, M., 2019. Phase 1 Study of Medi3902, an investigational anti-*Pseudomonas Aeruginosa* Pcrv and Psl bispecific human monoclonal antibody, in healthy adults. *Clin. Microbiol. Infect.* 25 <https://doi.org/10.1016/j.cmi.2018.08.004>, 629. e621–629. e626.
- Amnuakitt, T., Limsuwan, T., Khongkow, P., Boonme, P., 2018. Vesicular carriers containing phenylethyl resorcinol for topical delivery system; liposomes, transfersomes and invasomes. *Asian J. Pharm. Sci.* 13, 472–484. <https://doi.org/10.1016/j.ajps.2018.02.004>.
- Ansell, S.M., Harasym, T.O., Tardi, P.G., Buchkowsky, S.S., Bally, M.B., Cullis, P.R., 2000. Antibody conjugation methods for active targeting of liposomes. In: Francis, G. E., Delgado, C. (Eds.), *Drug Targeting: Strategies, Principles, and Applications*. Humana Press, Totowa, NJ, pp. 51–68. <https://doi.org/10.1385/1-59259-075-6:51>.
- Ascenso, A., Raposo, S., Batista, C., Cardoso, P., Mendes, T., Praça, F.G., Bentley, M.V.L. B., Simões, S., 2015. Development, characterization, and skin delivery studies of related ultradeformable vesicles: transfersomes, ethosomes, and transthesosomes. *Int. J. Nanomedicine* 5837–5851. <https://doi.org/10.2147/IJN.S86186>.
- Atawia, R.T., Mosli, H.H., Tadros, M.G., Khalifa, A.E., Mosli, H.A., Abdel-Naim, A.B., 2014. Modulatory effect of silymarin on inflammatory mediators in experimentally induced benign prostatic hyperplasia: emphasis on Pten, Hif-1 α , and Nf-Kb. *Naunyn Schmiedeberg's Arch. Pharmacol.* 387, 1131–1140. <https://doi.org/10.1007/s00210-014-1040-y>.
- Bale, S., Goebrecht, G., Stano, A., Wilson, R., Ota, T., Tran, K., Ingale, J., Zwick, M.B., Wyatt, R.T., 2017. Covalent linkage of Hiv-1 trimers to synthetic liposomes elicits improved B cell and antibody responses. *J. Virol.* 91 <https://doi.org/10.1128/jvi.00443-17>.
- Busetto, G.M., Giovannone, R., Ferro, M., Tricarico, S., Del Giudice, F., Matei, D.V., De Cobelli, O., Gentile, V., De Berardinis, E., 2014. Chronic bacterial prostatitis: efficacy of short-lasting antibiotic therapy with Prulifloxacin (Unidrox®) in Association with Saw Palmetto Extract, *Lactobacillus sporogens* and Arbutin (Lactorepens®). *BMC Urol.* 14, 1–9. <https://doi.org/10.1186/1471-2490-14-53>.
- Charalabopoulos, K., Karachalios, G., Baltogiannis, D., Charalabopoulos, A., Giannakopoulos, X., Sofikitis, N., 2003. Penetration of antimicrobial agents into the prostate. *Chemotherapy* 49, 269–279. <https://doi.org/10.1159/000074526>.
- Chen, M., Shamim, M.A., Shahid, A., Yeung, S., Andresen, B.T., Wang, J., Nekkanti, V., Meyskens Jr., F.L., Kelly, K.M., Huang, Y., 2020. Topical delivery of carvedilol Loaded nano-transfersomes for skin cancer chemoprevention. *Pharmaceutics* 12, 1151. <https://doi.org/10.3390/pharmaceutics1211151>.
- Cheng, Y., Cao, Y., Ihsan, A.U., Khan, F.U., Li, X., Xie, D., Cui, X., Wang, W., Liu, Z., Li, C., Ahmad, K.A., Sembatya, K.R., Mikrani, R., Zhou, X., 2019. Novel treatment of experimental autoimmune prostatitis by nanoparticle-conjugated autoantigen peptide T2. *Inflammation* 42, 1071–1081. <https://doi.org/10.1007/s10753-019-00968-5>.
- Cruz, L.J., Tacke, P.J., Fokkink, R., Figdor, C.G., 2011. The Influence of Peg chain length and targeting moiety on antibody-mediated delivery of nanoparticle vaccines to human dendritic cells. *Biomaterials* 32, 6791–6803. <https://doi.org/10.1016/j.biomaterials.2011.04.082>.
- Dalhoff, A., Weidner, W., 1988. Diffusion of ciprofloxacin into prostatic fluid. *Eur. J. Clin. Microbiol. Infect. Dis.* 7, 438–439. <https://doi.org/10.1007/BF01977495>.
- Davarpanah, F., Khalili Yazdi, A., Barani, M., Mirzaei, M., Torkezadeh-Mahani, M., 2018. Magnetic delivery of antitumor carboplatin by using pegylated-niosomes. *DARU J. Pharm. Sci.* 26, 57–64. <https://doi.org/10.1007/s40199-018-0215-3>.
- Edwards, K., Almgren, M., 1990. Kinetics of Surfactant-Induced Leakage and Growth of Unilamellar Vesicles, Surfactants and Macromolecules: Self-Assembly at Interfaces and in Bulk. Springer, pp. 190–197. <https://doi.org/10.1007/BFb0118258>.
- Ehi-Eromosele, C., Ita, B., Iweala, E., 2016. The effect of Polyethylene Glycol (Peg) coating on the magneto-structural properties and colloidal stability of Co₀.8mg₀.2fe_{2o4} nanoparticles for potential biomedical applications. *Dig. J. Nanomater. Biostruct.* 11, 7–14.
- El Meliegy, A.I., Torkey, M., 2015. An observational study to monitor the efficacy and tolerability of levofloxacin 500 mg once daily for treatment of chronic bacterial prostatitis in Saudi Arabia. *Urol. Annal.* 7, 71. <https://doi.org/10.4103/0974-7796.148623>.
- Elkahwaji, J., Hauke, R., Brawner, C., 2009. Chronic bacterial inflammation induces prostatic intraepithelial neoplasia in mouse prostate. *Br. J. Cancer* 101, 1740–1748. <https://doi.org/10.1038/sj.bjc.6605370>.
- El-Samalgly, M., Afifi, N., Mahmoud, E., 2006. Increasing bioavailability of silymarin using a buccal liposomal delivery system: preparation and experimental design investigation. *Int. J. Pharm.* 308, 140–148. <https://doi.org/10.1016/j.ijpharm.2005.11.006>.
- Elsenosy, F.M., Abdelbary, G.A., Elshafeey, A.H., Elsayed, I., Fares, A.R., 2020. Brain targeting of duloxetine Hcl via intranasal delivery of loaded cubosomal gel: in vitro characterization, ex vivo permeation, and in vivo biodistribution studies. *Int. J. Nanomedicine* 9517–9537. <https://doi.org/10.2147/IJN.S277352>.
- Fadeel, D.A.A., Kamel, R., Fadel, M., 2020. Pegylated lipid nanocarrier for enhancing photodynamic therapy of skin carcinoma using curcumin: in-vitro/in-vivo studies

- and histopathological examination. *Sci. Rep.* 10, 1–10. <https://doi.org/10.1038/s41598-020-67349-z>.
- Fang, J.-Y., Hong, C.-T., Chiu, W.-T., Wang, Y.-Y., 2001. Effect of liposomes and niosomes on skin permeation of enoxacin. *Int. J. Pharm.* 219, 61–72. [https://doi.org/10.1016/S0378-5173\(01\)00627-5](https://doi.org/10.1016/S0378-5173(01)00627-5).
- García-Fuentes, M., Torres, D., Alonso, M., 2003. Design of lipid nanoparticles for the oral delivery of hydrophilic macromolecules. *Colloids Surf. B: Biointerfaces* 27, 159–168. [https://doi.org/10.1016/S0927-7765\(02\)00053-X](https://doi.org/10.1016/S0927-7765(02)00053-X).
- García-Fuentes, M., Torres, D., Martín-Pastor, M., Alonso, M.J., 2004. Application of Nmr spectroscopy to the characterization of Peg-stabilized lipid nanoparticles. *Langmuir* 20, 8839–8845. <https://doi.org/10.1021/la049505j>.
- George, F.W., Griffin, J.E., Leshin, M., Wilson, J.D., 1981. Endocrine Control of Sexual Differentiation in the Human, Fetal Endocrinology. Elsevier, pp. 341–357. <https://doi.org/10.1016/B978-0-12-522601-1.50025-1>.
- Gregorio, D.I., Samociuk, H., DeChello, L., Swede, H., 2006. Effects of study area size on geographic characterizations of health events: prostate cancer incidence in Southern New England, USA, 1994–1998. *Int. J. Health Geogr.* 5, 1–8. <https://doi.org/10.1186/1476-072X-5-8>.
- Guo, H., Xu, Y.-M., Ye, Z.-Q., Yu, J.-H., 2012. Levels of Cytokines and Heat-shock Protein 70 in the seminal plasma of patients with chronic bacterial prostatitis and chronic prostatitis/chronic pelvic pain syndrome. *Zhonghua nan ke xue= Natl J. Androl.* 18, 1088–1092.
- Guy, R.H., Hadgraft, J., Taylor, M.J., Kellaway, I.W., 2011. Release of non-electrolytes from liposomes. *J. Pharm. Pharmacol.* 35, 12–14. <https://doi.org/10.1111/j.2042-7158.1983.tb04254.x>.
- Hadidi, N., Saffari, M., Faizi, M., 2018. Optimized Transfersomal Bovine Lactoferrin (Blf) as a promising novel non-invasive topical treatment for genital warts caused by Human Papilloma Virus (Hpv). *Iran. J. Pharm. Res.* 17, 12.
- Hassanpour, P., Hamishehkar, H., Baradaran, B., Mohammadi, M., Shomali, N., Spotin, A., Hazratian, T., Nami, S., 2020. An appraisal of antifungal impacts of nano-liposome containing voriconazole on voriconazole-resistant aspergillus flavus isolates as a groundbreaking drug delivery system. *Nanomed. Res. J.* 5, 90–100. <https://doi.org/10.22034/nmrj.2020.01.010>.
- Heath, T., Macher, B., Papahadjopoulos, D., 1981. Covalent attachment of immunoglobulins to liposomes via glycosphingolipids. *Biochim. Biophys. Acta (BBA)-Biomembr.* 640, 66–81. [https://doi.org/10.1016/0005-2736\(81\)90532-0](https://doi.org/10.1016/0005-2736(81)90532-0).
- Hochreiter, W.W., Duncan, J.L., Schaeffer, A.J., 2000. Evaluation of the bacterial flora of the prostate using a 16s Rrna gene based polymerase chain reaction. *J. Urol.* 163, 127–130. [https://doi.org/10.1016/S0022-5347\(05\)67987-6](https://doi.org/10.1016/S0022-5347(05)67987-6).
- Hosny, K.M., 2010. Ciprofloxacin as ocular liposomal hydrogel. *AAPS PharmSciTech* 11, 241–246. <https://doi.org/10.1208/s12249-009-9373-4>.
- Hu, R., Yang, Y., Song, G., Zhao, F., Chen, S., Zhou, Z., Zheng, J., Shen, W., 2022. In vivo targeting capacities of different nanoparticles to prostate tissues based on a mouse model of chronic bacterial prostatitis. *Front. Bioeng. Biotechnol.* 10 <https://doi.org/10.3389/fbioe.2022.1021385>.
- Hua, S., 2014. Comparison of in vitro dialysis release methods of loperamide-encapsulated liposomal gel for topical drug delivery. *Int. J. Nanomedicine* 735–744. <https://doi.org/10.2147/IJN.S55805>.
- Jain, A., Jain, S.K., 2016. In vitro release kinetics model fitting of liposomes: an insight. *Chem. Phys. Lipids* 201, 28–40. <https://doi.org/10.1016/j.chemphyslip.2016.10.005>.
- Jain, A.K., Kumar, F., 2017. Transfersomes: ultradeformable vesicles for transdermal drug delivery. *Asian J. Biomater.* Res 3, 1–3.
- Jain, S., Jain, P., Umamaheshwari, R., Jain, N., 2003. Transfersomes—a novel vesicular carrier for enhanced transdermal delivery: development, characterization, and performance evaluation. *Drug Dev. Ind. Pharm.* 29, 1013–1026. <https://doi.org/10.1081/DDC-120025458>.
- Jain, R., Beckett, V., Konstan, M., Accurso, F., Burns, J., Mayer-Hamblett, N., Milla, C., VanDevanter, D., Chmiel, J., Group, K.-A.S., 2018. Kb001-a, a Novel Anti-Inflammatory, Found to be Safe and Well-Tolerated in Cystic Fibrosis patients Infected with Pseudomonas Aeruginosa. *J. Cyst. Fibros.* 17, 484–491. <https://doi.org/10.1016/j.jcf.2017.12.006>.
- Jiang, J., Li, J., Yunxia, Z., Zhu, H., Liu, J., Pumill, C., 2013. The role of prostatitis in prostate cancer: meta-analysis. *PLoS One* 8. <https://doi.org/10.1371/journal.pone.0085179> e85179.
- Jiang, T., Wang, T., Li, T., Ma, Y., Shen, S., He, B., Mo, R., 2018. Enhanced transdermal drug delivery by transfersome-embedded oligopeptide hydrogel for topical chemotherapy of melanoma. *ACS Nano* 12, 9693–9701. <https://doi.org/10.1021/acsnano.8b03800>.
- Kamel, R., Abbas, H., Shaffie, N.M., 2019. Development and evaluation of pla-coated micellar nanosystem of resveratrol for the intra-articular treatment of arthritis. *Int. J. Pharm.* 569, 118560. <https://doi.org/10.1016/j.ijpharm.2019.118560>.
- Kashanian, S., Rostami, E., 2014. Peg-stearate coated solid lipid nanoparticles as levofloxacin carriers for oral administration. *J. Nanopart. Res.* 16, 1–10. <https://doi.org/10.1007/s11051-014-2293-6>.
- Khan, M.A., Pandit, J., Sultana, Y., Sultana, S., Ali, A., Aqil, M., Chauhan, M., 2015. Novel carbopol-based transfersomal gel of 5-fluorouracil for skin cancer treatment: in vitro characterization and in vivo study. *Drug Deliv.* 22, 795–802. <https://doi.org/10.3109/10717544.2014.902146>.
- Khan, M.I., Yaqoob, S., Madni, A., Akhtar, M.F., Sohail, M.F., Saleem, A., Tahir, N., Khan, K.-R., Qureshi, O.S., 2022. Development and in vitro/ex vivo evaluation of lecithin-based deformable transfersomes and transfersome-based gels for combined dermal delivery of meloxicam and dexamethasone. *Biomed. Res. Int.* 2022 <https://doi.org/10.1155/2022/8170318>.
- Kotla, N.G., Chandrasekar, B., Rooney, P., Sivaraman, G., Larrañaga, A., Krishna, K.V., Pandit, A., Rochev, Y., 2017. Biomimetic lipid-based nanosystems for enhanced dermal delivery of drugs and bioactive agents. *ACS Biomater. Sci. Eng.* 3, 1262–1272. <https://doi.org/10.1021/acsbomaterials.6b00681>.
- Kulkarni, V., Sonawane, L., 2017. Theoretical Exploration of Nanoparticles Targeting Bacterial Prostatitis.
- Le, H.N., Quetz, J.S., Tran, V.G., Le, V.T., Aguiar-Alves, F., Pinheiro, M.G., Cheng, L., Yu, L., Sellman, B.R., Stover, C.K., 2018. Medi3902 correlates of protection against severe Pseudomonas aeruginosa pneumonia in a rabbit acute pneumonia model. *Antimicrob. Agents Chemother.* 62 <https://doi.org/10.1128/aac.02565-17>.
- Le, H., Arnoult, C., Dé, E., Schapman, D., Galas, L., Le Cerf, D., Karakasyan-Dia, C., 2020. Antibody Conjugated Nanocarriers for Targeted Antibiotic delivery: Application in the Treatment of Bacterial Biofilm Infections. Available at SSRN 3737305. <https://doi.org/10.2139/ssrn.3737305>.
- Lei, W., Yu, C., Lin, H., Zhou, X., 2013. Development of tacrolimus-loaded transfersomes for deeper skin penetration enhancement and therapeutic effect improvement in vivo. *Asian J. Pharm. Sci.* 8, 336–345. <https://doi.org/10.1016/j.ajps.2013.09.005>.
- Li, T., Chen, L., Deng, Y., Liu, X., Zhao, X., Cui, Y., Shi, J., Feng, R., Song, Y., 2017. Cholesterol derivative-based liposomes for gemcitabine delivery: preparation, in vitro, and in vivo characterization. *Drug Dev. Ind. Pharm.* 43, 2016–2025. <https://doi.org/10.1080/03639045.2017.1361965>.
- Liu, C.-P., Chen, Z.-D., Ye, Z.-Y., He, D.-Y., Dang, Y., Li, Z.-W., Wang, L., Ren, M., Fan, Z.-J., Liu, H.-X., 2021. Therapeutic applications of functional nanomaterials for prostatitis. *Front. Pharmacol.* 12 <https://doi.org/10.3389/fphar.2021.685465>.
- Madan, J.R., Khude, P.A., Dua, K., 2014. Development and evaluation of solid lipid nanoparticles of mometasone furoate for topical delivery. *Int. J. Pharm. Invest.* 4, 60. <https://doi.org/10.4103/2F2230-973X.133047>.
- Manjunath, K., Reddy, J.S., Venkateswarlu, V., 2005. Solid lipid nanoparticles as drug delivery systems. *Methods Find. Exp. Clin. Pharmacol.* 27, 127–144. <https://doi.org/10.1358/mf.2005.27.2.876286>.
- McNeal, J.E., 1988. Normal histology of the prostate. *Am. J. Surg. Pathol.* 12, 619–633.
- Muppidi, K., Pumerantz, A.S., Wang, J., Betageri, G., 2012. Development and stability studies of novel liposomal vancomycin formulations. *Int. Schol. Res. Notices* 2012. <https://doi.org/10.5402/2012/636743>.
- Naber, K.G., 1989. Use of quinolones in urinary tract infections and prostatitis. *Rev. Infect. Dis.* 11, S1321–S1337. https://doi.org/10.1093/clinids/11.Supplement_5.S1321.
- Naber, K.G., Sörgel, F., Kees, F.K., Jaehde, U., Schumacher, H., 1989. Pharmacokinetics of ciprofloxacin in young (healthy volunteers) and elderly patients, and concentrations in prostatic fluid, seminal fluid, and prostatic adenoma tissue following intravenous administration. *Am. J. Med.* 87, S57–S59. [https://doi.org/10.1016/0002-9343\(89\)90023-5](https://doi.org/10.1016/0002-9343(89)90023-5).
- Nadler, R.B., Koch, A.E., Calhoun, E.A., Campbell, P.L., Pruden, D.L., Bennett, C.L., Yarnold, P.R., Schaeffer, A.J., 2000. Il-1 β and Tnf- α in prostatic secretions are indicators in the evaluation of men with chronic prostatitis. *J. Urol.* 164, 214–218. [https://doi.org/10.1016/S0022-5347\(05\)67497-6](https://doi.org/10.1016/S0022-5347(05)67497-6).
- Naik, S., Patel, D., Surti, N., Misra, A., 2010. Preparation of pegylated liposomes of docetaxel using supercritical fluid technology. *J. Supercrit. Fluids* 54, 110–119. <https://doi.org/10.1016/j.supflu.2010.02.005>.
- Nguyen, P.V., Herve-Aubert, K., Chourpa, I., Allard-Vannier, E., 2021. Active targeting strategy in nanomedicines using anti-Egfr ligands—a promising approach for cancer therapy and diagnosis. *Int. J. Pharm.* 609, 121134. <https://doi.org/10.1016/j.ijpharm.2021.121134>.
- Nickel, J.C., Roehrborn, C.G., O'Leary, M.P., Bostwick, D.G., Somerville, M.C., Rittmaster, R.S., 2008. The relationship between prostate inflammation and lower urinary tract symptoms: examination of baseline data from the reduce trial. *Eur. Urol.* 54, 1379–1384. <https://doi.org/10.1016/j.eururo.2007.11.026>.
- Okada, J., Asano, S., Kondo, T., 1991. A new concept for interpretation of first-order release from albumin microspheres. *J. Microencapsul.* 8, 483–496. <https://doi.org/10.3109/02652049109021872>.
- O'Shaughnessy, J.A., 2003. Pegylated liposomal doxorubicin in the treatment of breast cancer. *Clin. Breast Cancer* 4, 318–328. <https://doi.org/10.3816/CBC.2003.n.037>.
- Paget, G., Barnes, J., 1964. Chapter 6-Toxicity Tests, Evaluation of Drug Activities. Academic Press, Massachusetts, pp. 135–166.
- Pandey, A., Mittal, A., Chauhan, N., Alam, S., 2014. Role of surfactants as penetration enhancer in transdermal drug delivery system. *J. Mol. Pharm. Org Process Res.* 2, 2–7. <https://doi.org/10.4172/2329-9053.1000113>.
- Pena-Rodríguez, E., Moreno, M.C., Blanco-Fernandez, B., González, J., Fernández-Campos, F., 2020. Epidermal delivery of retinyl palmitate loaded transfersomes: penetration and biodistribution studies. *Pharmaceutics* 12, 112. <https://doi.org/10.3390/pharmaceutics12020112>.
- Penna, G., Mondaini, N., Amuchastegui, S., Degli Innocenti, S., Carini, M., Giubilei, G., Fibbi, B., Colli, E., Maggi, M., Adorini, L., 2007. Seminal plasma cytokines and chemokines in prostate inflammation: interleukin 8 as a predictive biomarker in chronic prostatitis/chronic pelvic pain syndrome and benign prostatic hyperplasia. *Eur. Urol.* 51, 524–533. <https://doi.org/10.1016/j.eururo.2006.07.016>.
- Pfau, A., 1986. Prostatitis: a Continuing Enigma. *Urol. Clin. N. Am.* 13, 695–715. [https://doi.org/10.1016/S0094-0143\(21\)00273-1](https://doi.org/10.1016/S0094-0143(21)00273-1).
- Rahman, I., Gilmour, P.S., Jimenez, L.A., MacNee, W., 2002. Oxidative stress and Tnf- α induce histone acetylation and Nf-Kb/Ap-1 activation in alveolar epithelial cells: potential mechanism in gene transcription in lung inflammation. *Oxygen/nitrogen radicals. Cell Injury Dis.* 239–248. https://doi.org/10.1007/978-1-4615-1087-1_28.
- Rahmi, A.D., Pangesti, D.M., 2018. Comparison of the characteristics of transfersomes and protransfersomes containing azelaic acid. *J. Young Pharm.* 10, S11.
- Rajan, R., Jose, S., Mukund, V.B., Vasudevan, D.T., 2011. Transfersomes—a vesicular transdermal delivery system for enhanced drug permeation. *J. Adv. Pharm. Technol. Res.* 2, 138. <https://doi.org/10.4103/2231-4040.85524>.

- Ramana, L.N., Sharma, S., Sethuraman, S., Ranga, U., Krishnan, U.M., 2012. Investigation on the stability of saquinavir loaded liposomes: implication on stealth, release characteristics and cytotoxicity. *Int. J. Pharm.* 431, 120–129. <https://doi.org/10.1016/j.ijpharm.2012.04.054>.
- Reznik, G., Hamlin, M.H., Ward, J.M., Stinson, S.F., 1981. Prostatic hyperplasia and neoplasia in aging F344 rats. *Prostate* 2, 261–268. <https://doi.org/10.1002/pros.2990020304>.
- Sachan, R., Parashar, T., Soniya, S.V., Singh, G., Tyagi, S., Patel, C., Gupta, A., 2013. Drug carrier transfersomes: a novel tool for transdermal drug delivery system. *In. J. Res. Dev. Pharm. Life Sci.* 2, 309–316.
- Santamaria, S., de Groot, R., 2019. Monoclonal antibodies against metzincin targets. *Br. J. Pharmacol.* 176, 52–66. <https://doi.org/10.1111/bph.14186>.
- Santharam, M.A., Khan, F.U., Naveed, M., Ali, U., Ahsan, M.Z., Khongorzul, P., Shoaib, R. M., Ihsan, A.U., 2019. Interventions to chronic prostatitis/chronic pelvic pain syndrome treatment. where are we standing and what's next? *Eur. J. Pharmacol.* 857, 172429. <https://doi.org/10.1016/j.ejphar.2019.172429>.
- Shehata, T., Kimura, T., Higaki, K., Ogawara, K.-i, 2016. In-vivo disposition characteristics of peg niosome and its interaction with serum proteins. *Int. J. Pharm.* 512, 322–328. <https://doi.org/10.1016/j.ijpharm.2016.08.058>.
- Shulyak, A., Gorpynchenko, L., Drannik, G., Poroshina, T., Savchenko, V., Nurimanov, K., 2019. The effectiveness of the combination of rectal electrostimulation and an antidepressant in the treatment of chronic abacterial prostatitis. *Centr. Eur. J. Urol.* 72, 66. <https://doi.org/10.5173/cej.2018.1719>.
- Sinha, M., Banik, R.M., Haldar, C., Maiti, P., 2013. Development of ciprofloxacin hydrochloride loaded poly (ethylene glycol)/chitosan scaffold as wound dressing. *J. Porous. Mater.* 20, 799–807. <https://doi.org/10.1007/s10934-012-9655-1>.
- Sivannarayana, P., Rani, A.P., Saikishore, V., VenuBabu, C., SriRekha, V., 2012. Transfersomes: ultra deformable vesicular carrier systems in transdermal drug delivery System. *Res. J. Pharm. Dosage Forms Technol.* 4, 243–255.
- Szoka, F., Papahadjopoulos, D., 1978. Procedure for preparation of liposomes with large internal aqueous space and high capture by reverse-phase evaporation. *Proc. Natl. Acad. Sci.* 75, 4194–4198. <https://doi.org/10.1073/pnas.75.9.4194>.
- Talsma, H., Crommelin, D., 1993. Liposomes as drug delivery systems. Iii: Stabilization. *Pharm. Technol.* 17, 48.
- Torchilin, V., 1998. Polymer-coated long-circulating microparticulate pharmaceuticals. *J. Microencapsul.* 15, 1–19. <https://doi.org/10.3109/02652049809006831>.
- Valenta, C., Wanka, M., Heidlas, J., 2000. Evaluation of novel soya-lecithin formulations for dermal use containing ketoprofen as a model drug. *J. Control. Release* 63, 165–173. [https://doi.org/10.1016/S0168-3659\(99\)00199-6](https://doi.org/10.1016/S0168-3659(99)00199-6).
- Vikas, K., Arvind, S., Ashish, S., Gourav, J., Vipasha, D., 2011. Recent advances in Ndds (novel drug delivery system) for delivery of anti-hypertensive drugs. *Int. J. Drug Dev. Res.* 3, 252–259.
- Visan, L., Rouleau, N., Proust, E., Peyrot, L., Donadieu, A., Ochs, M., 2018. Antibodies to Pcpa and Phtd protect mice against *Streptococcus pneumoniae* by a macrophage-and complement-dependent mechanism. *Hum. Vaccin. Immunother.* 14, 489–494. <https://doi.org/10.1080/21645515.2017.1403698>.
- Walve, J., Bakliwal, S., Rane, B., Pawar, S., 2011. Transfersomes: A Surrogated Carrier for Transdermal Drug Delivery System.
- Wang-Lin, S.X., Balthasar, J.P., 2018. Pharmacokinetic and pharmacodynamic considerations for the use of monoclonal antibodies in the treatment of bacterial infections. *Antibodies* 7, 5. <https://doi.org/10.3390/antib7010005>.
- Xiong, S., Liu, X., Deng, W., Zhou, Z., Li, Y., Tu, Y., Chen, L., Wang, G., Fu, B., 2020. Pharmacological interventions for bacterial prostatitis. *Front. Pharmacol.* 11, 504. <https://doi.org/10.3389/fphar.2020.00504>.
- Xue, W., Trital, A., Shen, J., Wang, L., Chen, S., 2020. Zwitterionic polypeptide-based nanodrug augments Ph-triggered tumor targeting via prolonging circulation time and accelerating cellular internalization. *ACS Appl. Mater. Interfaces* 12, 46639–46652. <https://doi.org/10.1021/acsami.0c11747>.
- Zeb, A., Qureshi, O.S., Kim, H.-S., Cha, J.-H., Kim, H.-S., Kim, J.-K., 2016. Improved skin permeation of methotrexate via nanosized ultradeformable liposomes. *Int. J. Nanomedicine* 3813–3824. <https://doi.org/10.2147/IJN.S109565>.
- Zhang, D., Zhang, J., 2020. Surface engineering of nanomaterials with phospholipid-polyethylene glycol-derived functional conjugates for molecular imaging and targeted therapy. *Biomaterials* 230, 119646. <https://doi.org/10.1016/j.biomaterials.2019.119646>.
- Zhang, Y., Long, M., Huang, P., Yang, H., Chang, S., Hu, Y., Tang, A., Mao, L., 2016. Emerging integrated nanoclay-facilitated drug delivery system for papillary thyroid cancer therapy. *Sci. Rep.* 6, 33335. <https://doi.org/10.1038/srep33335>.
- Zhao, L., Temelli, F., Curtis, J.M., Chen, L., 2015. Preparation of liposomes using supercritical carbon dioxide technology: effects of phospholipids and sterols. *Food Res. Int.* 77, 63–72. <https://doi.org/10.1016/j.foodres.2015.07.006>.
- Zheng, J., Hu, R., Yang, Y., Wang, Y., Wang, Q., Xu, S., Yao, P., Liu, Z., Zhou, J., Yang, J., 2022. Antibiotic-loaded reactive oxygen species-responsive nanomedicine for effective management of chronic bacterial prostatitis. *Acta Biomater.* 143, 471–486. <https://doi.org/10.1016/j.actbio.2022.02.044>.